

## Lithospheric flexure and bending of the Central Andes

A.B. Watts<sup>a</sup>, S.H. Lamb<sup>a</sup>, J.D. Fairhead<sup>b</sup>, J.F. Dewey<sup>a</sup>

<sup>a</sup> *Department of Earth Sciences, Parks Road, Oxford OX1 3PR, UK*

<sup>b</sup> *GETECH, Department of Earth Sciences, Leeds LS2 9JT, UK*

Received 28 December 1994; accepted 11 May 1995

---

### Abstract

Gravity anomaly and topography data are used to define the effective elastic thickness of the lithosphere,  $T_e$ , in the bend region of the Central Andes. Values of  $T_e$  increase from nearly zero, north and south of the bend, to values greater than 50 km at the bend in Bolivia. There is a close correlation between  $T_e$  and the style and magnitude of the shortening in the Central Andes since the Late Miocene. In the bend region, where the lithosphere is flexurally strong with large  $T_e$ , foreland deformation is concentrated into a thin-skinned fold-and-thrust belt above a basal décollement which has absorbed more than 100 km of shortening. Further north and south, where the lithosphere is flexurally weak with low  $T_e$ , foreland deformation is more complex, involves basement and has absorbed less shortening. The along-strike gradients in foreland shortening have accommodated both clockwise and anticlockwise rotations about a vertical axis of almost the entire width of the Bolivian Andes. We speculate that the observed variation in  $T_e$  is related to the proximity of the Brazilian shield and has been an important factor in controlling the nature and amount of foreland deformation, and hence bending of the Central Andes. The flexural properties of the lithosphere may play an important role in determining the large-scale evolution of mountain belts.

---

### 1. Introduction

The association of mountain belts with thick crust and small-amplitude free-air gravity anomalies [1] suggest that they are in some form of isostatic equilibrium. The Airy model of 'local' isostasy successfully predicts the crustal thickness and gravity anomaly over the central parts of many mountain belts [2]. However, departures from Airy near their edges indicate that mountain belts may be compensated more regionally by flexure [3–5]. Recent models of mountain belt formation, which analyse continental deformation in terms of large-scale lithospheric flow [6,7], assume that such departures from an Airy model do not significantly influence the pattern of large-scale deformation.

The Andes form one of the world's largest mountain belts, and are up to 6500 m high, 600 km wide and 5000 km long (Fig. 1). They are the result of the subduction of the Nazca (or Farallon) Plate since the Cretaceous beneath the South American Plate along the Peru–Chile Trench. In the Central Andes, active plate convergence is in a roughly east–west direction at ca. 85 mm/yr (NUVEL-1, [8]). Here, the Andes are highest and widest, with a broad 200 km wide central plateau (Altiplano) at a general altitude of 4000 m, bounded by the Eastern and Western Cordilleras. The Western Cordillera follows the active volcanic arc. Active surface deformation is concentrated along the eastern margin of the Andes in the thin-skinned Sub-Andean fold-and-thrust belt [9]. A striking feature of the Central Andes is the abrupt

change in the trend of the mountain belt in Bolivia [10], from ca. northwest–southeast north of the bend to ca. north–south further south.

Previous studies of the gravity field of the Andes [4,11,12] have focused on the interpretation of individual profiles, rather than considering the state of

isostasy *along* the mountain belt. The main exception has been the work of Whitman [13] who has proposed that the flexural strength of the lithosphere that underlies the Sub-Andean basins increases northward in the region that is south of bend. A problem with these studies is that they have mainly

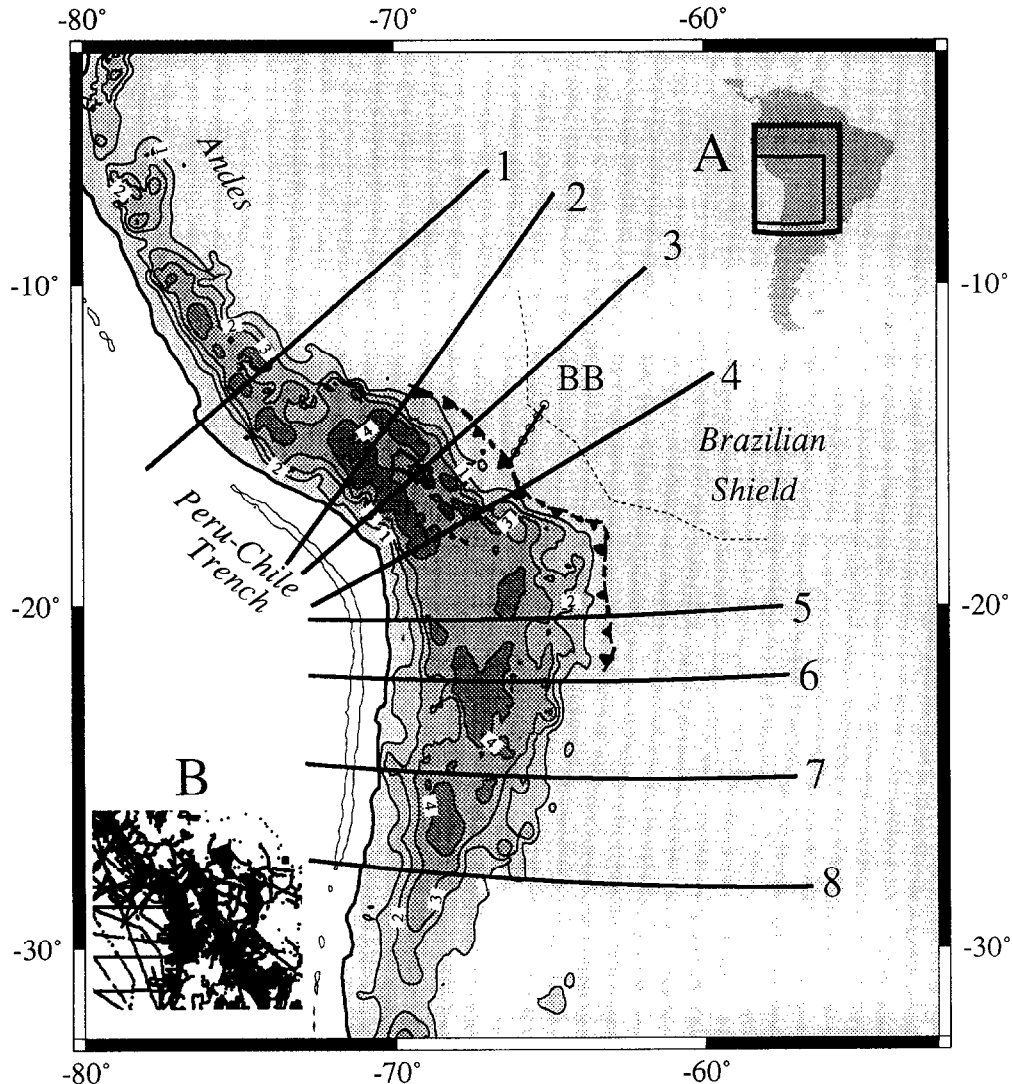


Fig. 1. Location map showing the topography of the bend region of the Central Andes. The topography data have been contoured at 1 km intervals. Offshore, the Peru–Chile trench axis is defined by the 6 km depth contour. Profiles 1–8 show the location of the topography and Bouguer gravity anomaly profiles in Fig. 2. The barbed line is the frontal thrust that bounds the eastern extent of the Sub-Andean fold-and-thrust belt. The finely stippled area shows the present-day outcrop pattern of the Brazilian shield [11]. *BB* = Location of the unpublished seismic reflection profile over the Beni Basin (cf. Fig. 5). *Inset A*: Location map of the bend region; outer box shows the study area; inner box shows the location of the data distribution map in inset *B*. *Inset B*: Distribution of the smoothed  $2.5 \times 2.5$  minute Bouguer gravity anomaly values in the bend region.

been based on a dataset compiled by the Defence Mapping Agency (DMA) which is particularly sparse in the Sub-Andean region where flexure is likely to be important. In this paper, we use a new compila-

tion of gravity anomaly and topography data, which includes all the available government, academic and commercial data, to define the long-term flexural strength of the lithosphere in the Sub-Andean region.

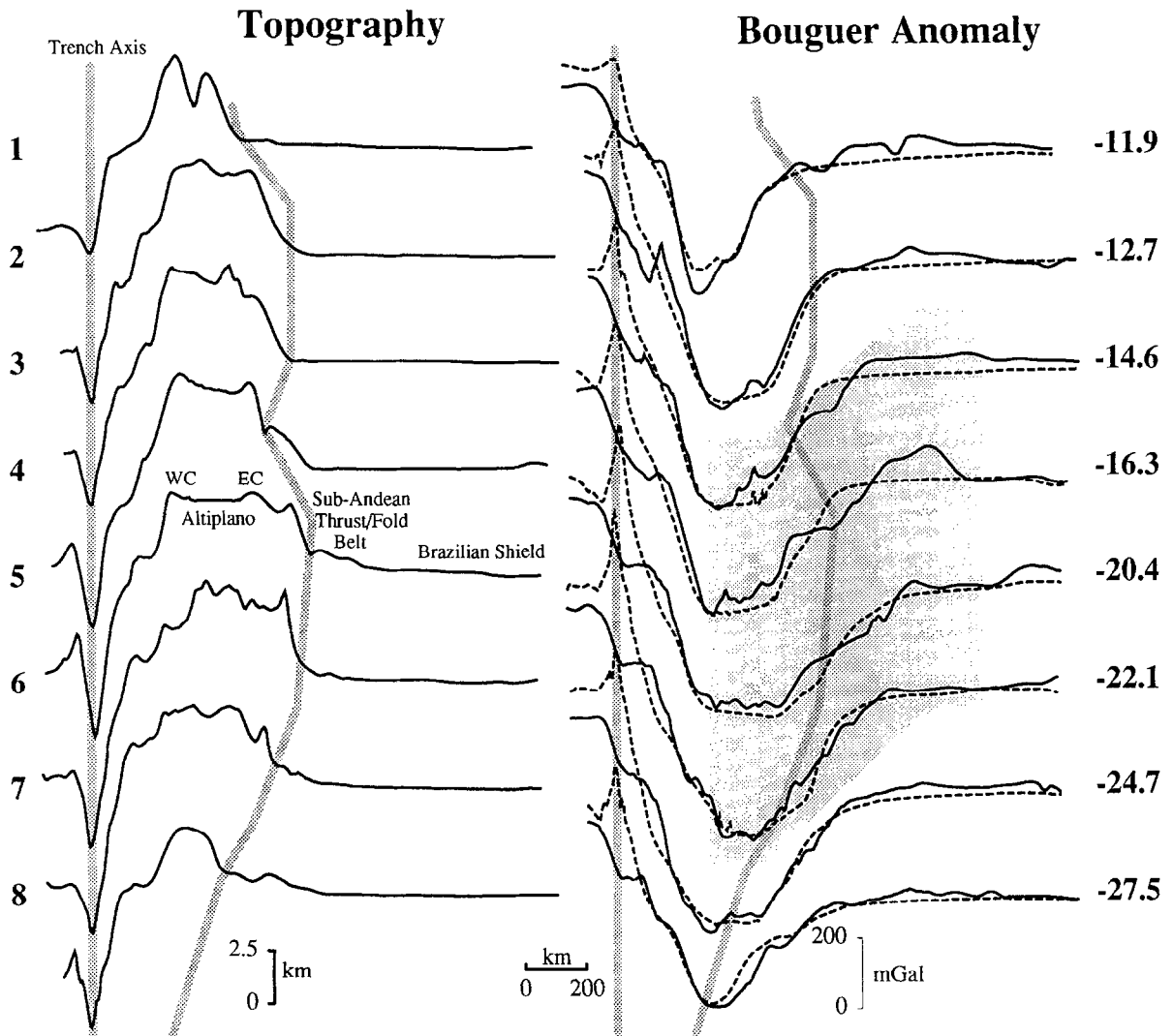


Fig. 2. Topography and Bouguer gravity anomaly Profiles 1–8 (Fig. 1) across the bend region. The profiles have been constructed from a  $5 \times 5$  minute grid of the smoothed gravity anomaly and topography data and have been aligned on the axis of the Peru–Chile trench. The dashed line is the Bouguer anomaly that would be predicted if the excess elevation of the Central Andes region was compensated by a deep crustal ‘root’ as predicted by a ‘hidden-layer’ Airy-type model [3]. The calculations assume a zero elevation thickness of the crust of 31.2 km and uniform densities of 2800, 2900 and  $3330 \text{ kg m}^{-3}$  for the upper crust, lower crust and mantle respectively. The right-hand grey lines delineate the topographic break in slope between the Eastern Cordillera and the Sub-Andean thrust-and-fold belt. The shaded region marks the parts of the Bouguer gravity anomaly profiles (3–6) shown in Fig. 3. The numbers to the left of the topography profiles are the profile numbers, those to the right of the Bouguer anomaly profiles the approximate latitude (degrees) of the profile mid-points.

We use the results to investigate the possible influence of variations in this flexural strength on the geological development of this region.

## 2. Data

Selected topography and gravity anomaly profiles from the Central Andes Bend region are shown in Fig. 2. The profiles were constructed from the compilation of topography and Bouguer gravity anomaly data carried out by the University of Leeds as part of its South America Gravity Project (SAGP) [14].

The SAGP dataset includes all the available government, commercial and academic ‘point’ measurements (Fig. 1, inset). Individual free-air gravity anomalies have been corrected for ‘rogue’ points or ‘outliers’, errors in base station tie-ins, and intersurvey incompatibility. The anomalies have also been corrected for the gravity effect of variations in the terrain around a measurement point. Where terrain corrections had been previously computed to 100 km or more from a point measurement these values were used; otherwise terrain corrections were recomputed to an ‘outer zone’ of 166.7 km. The reduction to Bouguer anomaly was carried out using a 3D terrain model and a uniform reduction density of  $2700 \text{ kg m}^{-3}$ . The final data processing step was to smooth each Bouguer anomaly value over a  $2.5 \times 2.5$  minute ‘square’ and then grid the values at  $5 \times 5$  minute intervals using a minimum curvature technique [15].

Fig. 2 shows that the Altiplano region of the Central Andes correlates with a broad, large-amplitude, Bouguer gravity anomaly ‘low’. The low reaches wavelengths of up to 1000 km and amplitudes of up to 400 mGal, which we interpret as a consequence of thick crust in the region between the Brazilian shield to the east and the Peru–Chile trench fore-arc region to the west. There is evidence (especially on Profiles 2–4) that the Bouguer anomaly minima is offset to the west such that the Eastern Cordillera correlates with a higher amplitude Bouguer anomaly than the Western Cordillera. The broad, large-amplitude Bouguer anomaly ‘high’ observed in offshore regions reflects a decrease in crustal thickness towards the trench.

The dashed line in Fig. 2 shows the Bouguer anomaly that would be expected if the Andes were

compensated by a deep crustal root as predicted by the Airy model. There is general agreement between calculated and observed Bouguer anomaly profiles over the Western Cordillera and Altiplano. A persistent difference occurs, however, between observed and calculated anomalies in the trench region. This is because the calculated anomalies are based on a Fast Fourier Transform technique which assumes a similar density for the oceanic and continental loads. However, this ‘artefact’ does not concern us here, as the area of interest in this paper is further to the east in the Eastern Cordillera and Sub-Andean zone. A more significant difference between observed and calculated gravity anomalies occurs in the region of the topographic ‘break in slope’ between the Eastern Cordillera and the Sub-Andean thrust belt. The difference is particularly well seen on Profiles 3–6 in the bend region, which show that it has the form of a positive–negative ‘couple’ with the observed being more *positive* than the calculated over the flanks of the Eastern Cordillera and more *negative* over the Sub-Andean fold-and-thrust belt. The positive–negative couple *could* be caused by density differences in the underlying basement but is more easily, we believe, interpreted in terms of lithospheric flexure.

## 3. Interpretation

To better evaluate the role of flexure, we have compared the observed Bouguer gravity anomaly in the bend region with calculated anomalies based on a 3D infinite elastic plate model. The model assumes that the South American lithosphere responds to long-term ( $> 10^6$  yr) loads as an elastic plate floating on a weak fluid substratum. Topography produces a surface load that deforms the elastic plate by an amount that depends on the geometry of the load, its density structure and the effective elastic thickness ( $T_e$ ) of the lithosphere. The gravity field is sensitive to the mass distributions associated with the load and its deformation and so can be used to constrain  $T_e$ . Small values of  $T_e$  ( $T_e \sim 0$  km) imply that the deformation of the lithosphere approaches that predicted by the Airy model, with local isostatic compensation. However, larger values of  $T_e$  ( $T_e > 0$  km) suggest that the lithosphere has a marked flexural rigidity. The effect of flexure is to spread the

deformation due to the surface loads (topography) of the Andes over a broader region. As Fig. 3 shows, this results in a calculated gravity anomaly that is more positive over the Eastern Cordillera and more negative over the fold-and-thrust belt than would be

predicted by an Airy model and that is, therefore, in better agreement with the data.

Although there are still a number of short-wavelength Bouguer anomalies in the observed profiles which cannot be explained, Fig. 3 shows that the

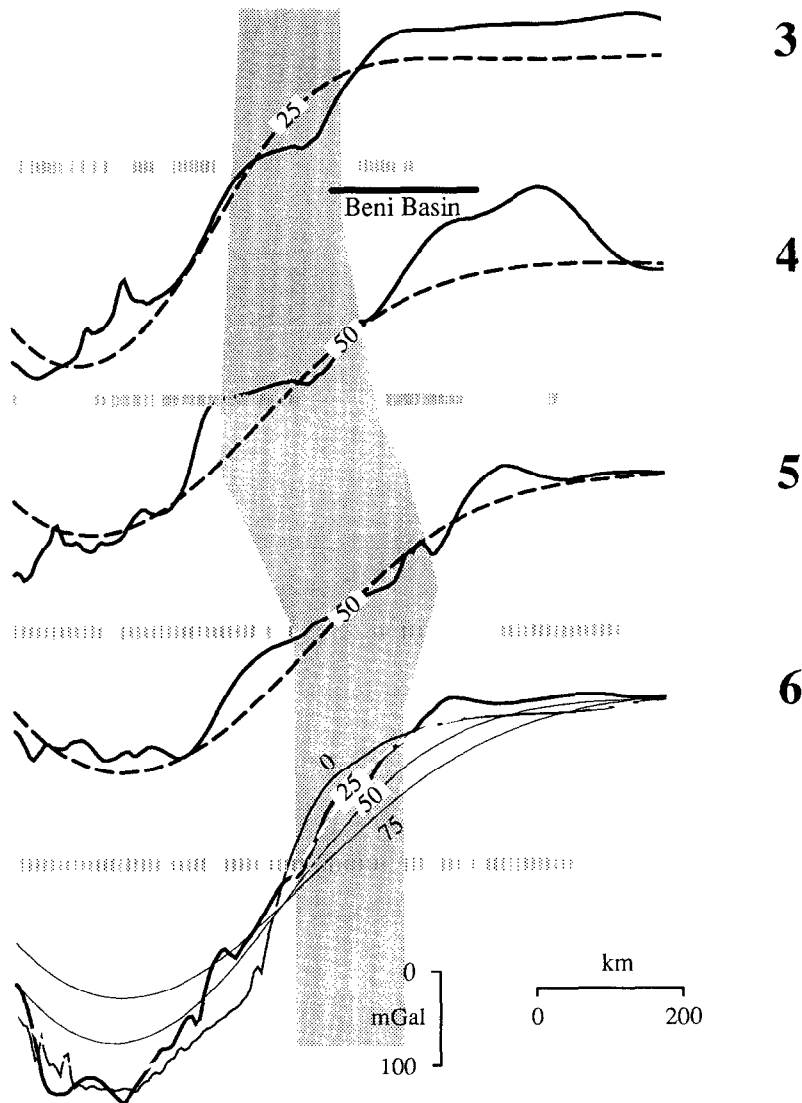


Fig. 3. Comparison of observed Bouguer gravity anomaly profiles (solid line) with calculated profiles (heavy dashed lines) based on an elastic plate model. The numbers on each best-fitting profile indicate the best-fitting elastic thickness. The light lines on Profile 6 show the calculated profiles for  $T_e$  of 0, 50 and 75 km. The root mean square differences between the observed and calculated gravity anomaly based on the best-fitting  $T_e$  along Profiles 3, 4, 5 and 6 are 28.9, 35.3, 20.9 and 14.0 respectively. The calculations assume Young's modulus of 100 GPa, Poisson's ratio of 0.25, and a load and infill density of  $2700 \text{ kg m}^{-3}$ . The vertical grey bars show the distribution of the  $2.5 \times 2.5$  'smoothed' values that are located within a 'window' 15 km either side of each profile, and the spacing between individual bars indicates the data coverage in the immediate vicinity of each profile. The region shaded grey shows the approximate extent of the Sub-Andean fold-and-thrust belt.

## Regional Isostatic Gravity Anomalies

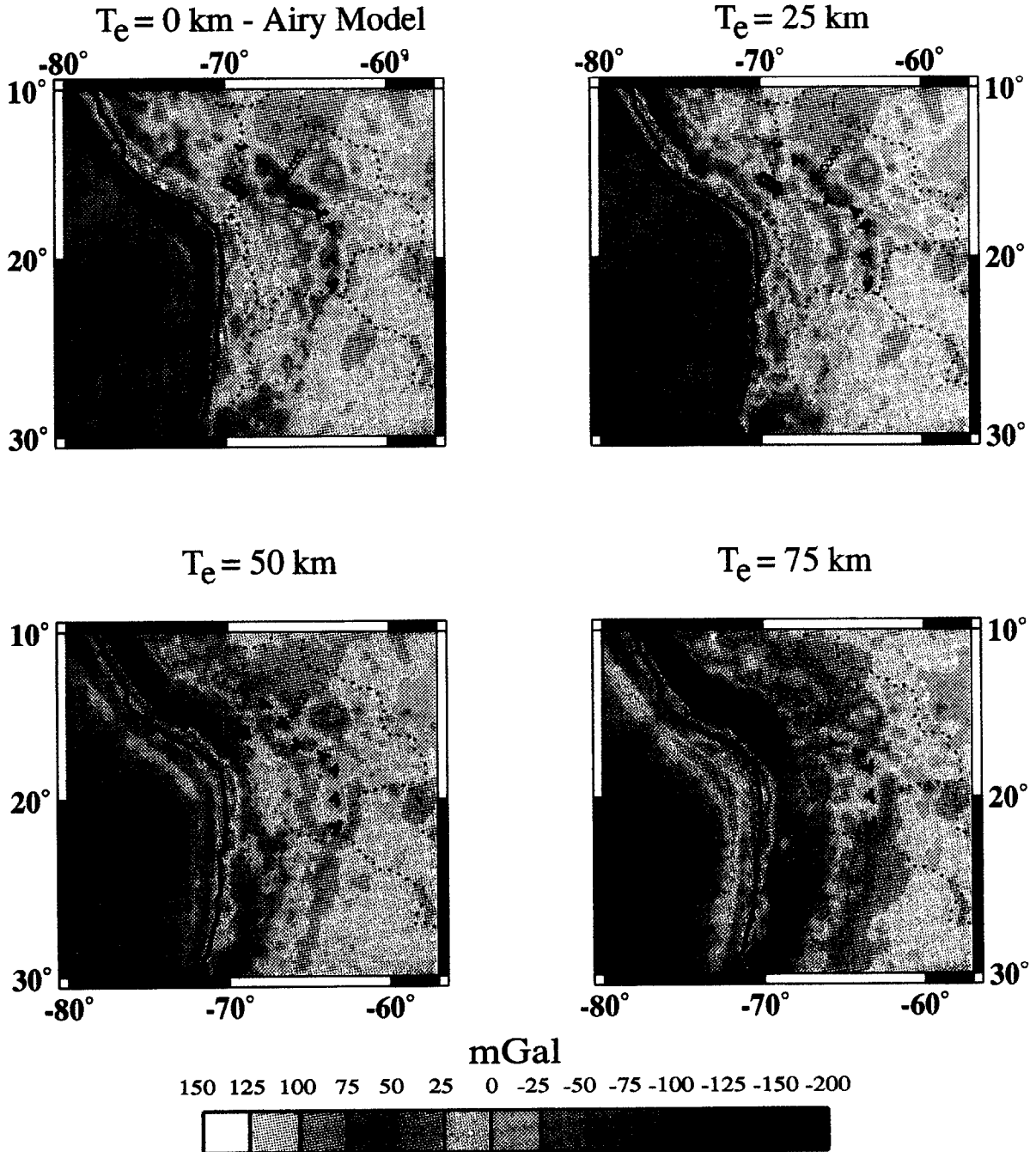


Fig. 4. Regional isostatic gravity anomaly maps of the bend region. The maps have been constructed by subtracting the gravity effect of the compensation of the topographic loads of the Andes from the observed Bouguer gravity anomaly. The compensation has been computed assuming that the Andes represent a load on the surface of a 3D continuous elastic plate for different values of the elastic thickness of the lithosphere ( $T_e$  of 0, 25, 50 and 75 km). The barbed line is the frontal thrust that bounds the eastern extent of the Sub-Andean fold-and-thrust belt and the line of circles is the Beni Basin profile. The difference in the general level of the isostatic anomalies between oceans and continents is an artefact of the Fast Fourier Transform method used to compute the gravity effect and arises because the same density has been assumed for the upward-acting loads of the oceans as was used for the downward-acting loads of the continents.

long wavelengths of each profile can generally be accounted for by flexure. The ‘best-fit’ for Profiles 3 and 6 is a  $T_e$  of 25 km, which increases to greater

than 50 km for Profiles 4 and 5. Sensitivity studies show that Profiles 3 and 6 could be explained by a  $T_e$  of less than 25 km while Profiles 4 and 5 require  $T_e$

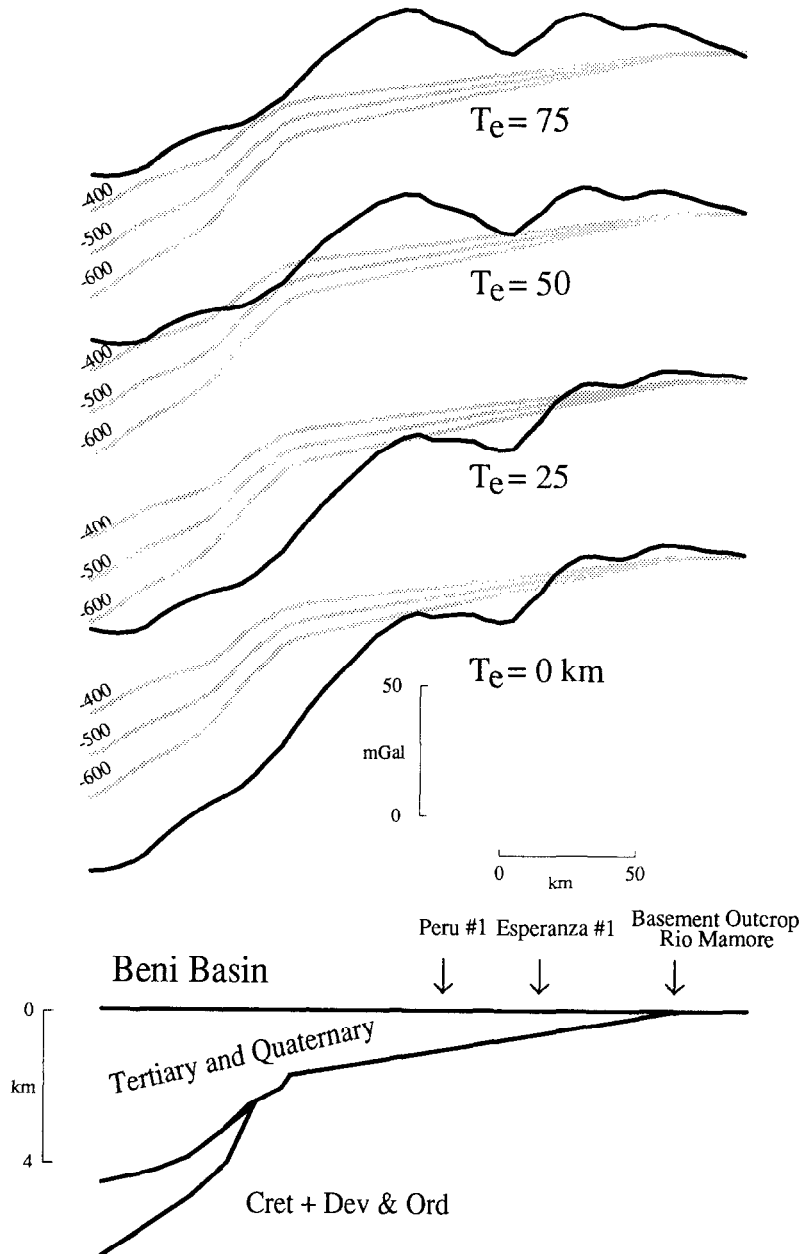


Fig. 5. Comparison of the ‘observed’ isostatic gravity anomalies with calculated anomalies along a profile across the Beni Basin. The observed anomalies are based on values of  $T_e$  of 0, 25, 50 and 75 km (heavy lines). The calculated anomalies assume density contrasts between sediments and basement rocks of 400, 500 and 600  $\text{kg m}^{-3}$  and a basin geometry (lower profile) that is defined by the available commercial seismic and well data. The figure shows that the best overall fit between the observed and calculated anomalies is for  $T_e$  between 25 and 50 km.

values of at least 50 km to explain them. These values, when taken with the absence of a positive–negative anomaly couple on the profiles to the north and south of the bend region (Fig. 2), suggest that  $T_e$  is high in the bend region and that it decreases to the north and south.

In the calculations involved in Fig. 3, we have assumed that the only loads acting on the plate are from the thrust and fold loads that make up the surface topography. We have therefore ignored the effects of any ‘buried’ (i.e., subsurface) [3] or ‘dynamic’ loads [16] that may have acted on the lithosphere during plate convergence. The Eastern Cordillera is associated with a somewhat higher Bouguer anomaly than is expected for its elevation, which might suggest a buried load. However, the Andes are not associated with a large-amplitude Bouguer gravity high of the type that characterises the Appalachian and Alpine orogenic belts where buried loads have been inferred [3]. We do not believe, therefore, that buried loads have contributed significantly to the gravity field or flexure along the Andean foldbelt. The Andes are located in a region of active seismicity, volcanism and deep thrust-fault earthquakes and, therefore, the possibility of dynamic loads cannot be ruled out. Such loads would be most likely a consequence of shear traction on the base of the South American Plate resulting from subduction of the Nazca Plate, and should change with variations in the subduction geometry. However, such changes in the geometry of the subducted plate [16,17] appear to be very long wavelength (up to 1600 km) and we do not believe that they have contributed in a major way to the short-wavelength features of Sub-Andean basin flexure.

Although the profiles in Fig. 3 provide useful information on the flexural rigidity of the bend region, they are limited to single ‘transects’ of the foreland basin lithosphere. A better way to investigate any spatial variations that may occur in the flexural rigidity throughout the bend region is through studies of the isostatic anomaly maps, especially ones that are based on the flexure model. Fig. 4 shows, for example, a set of isostatic anomaly maps for the bend region. The map based on  $T_e = 0$  km (i.e., Airy), for example, shows small-amplitude isostatic anomalies to the north and south of the bend, indicating that these regions are fully compensated.

Within the bend region, however, a low  $T_e$  produces large-amplitude *positive* isostatic anomalies, which show a correlation with topography. The existence of positive isostatic anomalies indicates under-compensation and, therefore, that the depth to the Moho and the thickness of the crust must be less than the  $T_e = 0$  model would predict. The  $T_e = 75$  km case, on the other hand, shows large-amplitude *negative* anomalies in the bend region, indicating over-compensation and thicker crust than in the  $T_e = 75$  km model. The only  $T_e$  values that show nearly zero isostatic anomalies in the bend region are intermediate in value and correspond to  $T_e = 25$ –50 km. In contrast, nearly zero anomalies to the north and south of the bend region occur for the 0 and 25 km case, confirming that  $T_e$  increases toward the bend region.

Further evidence for a high  $T_e$  in the bend region comes from a comparison of the gravity ‘lows’ based on different isostatic models over sedimentary basins to the anomalies that would be expected based on the thickness of sediments in these basins. One example of these is the gravity ‘low’ (Fig. 4) which correlates with the Beni Basin. Unpublished oil company seismic and well data indicate that this basin is underlain by up to 7 km of mainly Tertiary and younger sediments which overlie basement rocks of the Brazilian shield. Fig. 5 shows that the amplitude of the ‘low’ increases from about 30 mGal for  $T_e = 75$  km, to 50 mGal for  $T_e = 50$  km and to 100 mGal for  $T_e = 0$  km. The gravity low *expected* from the basin infill is about 50 mGal, assuming a uniform density contrast of  $-400 \text{ kg m}^{-3}$  between sediments and basement rocks, suggesting that a  $T_e$  value of 50 km is a good description of the background ‘regional’ gravity field of the Beni Basin region.

A criticism of our flexural modelling could be made because an infinite (i.e., continuous), rather than a semi-infinite (i.e., fractured), elastic plate model has been used to compute foreland basin flexure. Although Jordan [18] and Beaumont [19] used continuous plate models in their studies, previous studies of the Central Andes region [4] have used a fractured model. A similar model was used by Hanks [20] for the Kuril deep-sea trench–island-arc system and is considered, generally, an appropriate one to use when modelling regions where one plate is being underthrust by another. A problem in apply-

ing the model to orogenic belts is identification of where to locate the plate fracture. If we assume a location of the plate fracture (i.e., 200 km from the outermost thrust) similar to that used by Lyon-Caen and Molnar [4], then, as Fig. 6 shows, the effect of a fractured compared to a continuous plate model is to produce more flexure for the same load and for the

distance to the peripheral bulges to decrease. However, as is also shown in Fig. 6,  $T_e$  has to be *higher* to compensate for these changes. Thus, our conclusion that  $T_e$  increases in the bend region is unaffected, but we caution that, like other studies, our estimates are model-dependent and, therefore, may be only minimum estimates.

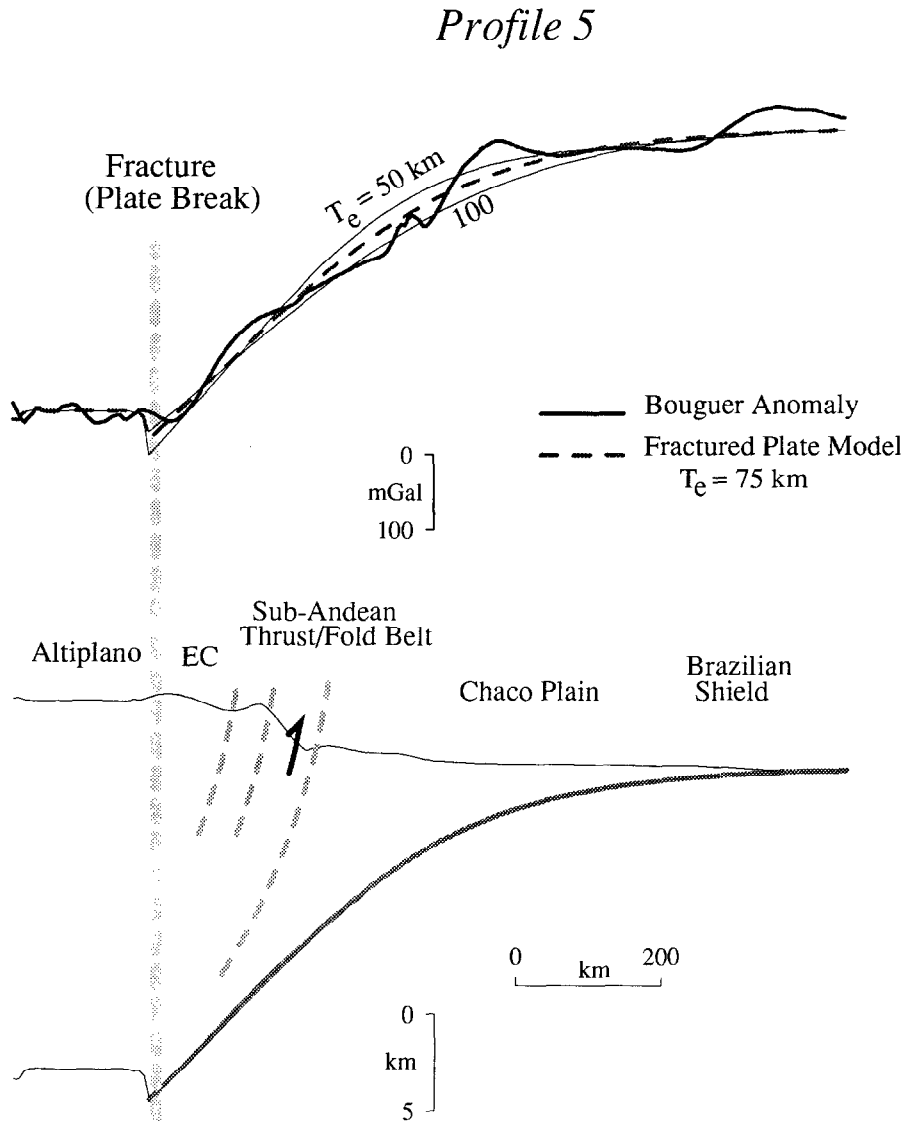


Fig. 6. Comparison of observed Bouguer gravity anomaly Profile 5 (heavy line) with calculations based on a fractured plate model with  $T_e$  of 50 km (light line), 75 km (dashed line) and 100 km (light line). The best overall fit to the observed profile is for  $T_e = 75$  km. The vertical dashed line shows the assumed location of the 'plate break', approximately 200 km west of the thrust-and-fold belt front. The lower profile is a schematic diagram showing the structure the Sub-Andean thrust-and-fold belt, the adjacent foreland basin and the Brazilian shield. The heavy grey line shows the predicted flexure of the Brazilian shield based on a fractured plate model with  $T_e = 75$  km.

#### 4. Discussion

This study of gravity anomaly and topography data suggests a regional variation in the flexural rigidity of the South American lithosphere. However, the particular value of  $T_e$  that ensures the 'best fit' with observed gravity anomalies along individual profiles was calculated for a 3D infinite elastic plate with a uniform value of  $T_e$ . Therefore, although we believe that, in reality,  $T_e$  varies smoothly with position, both in a north–south and east–west direction, it is not possible to determine unambiguously this variation from the results presented here. If it is assumed that the  $T_e$  value calculated for each profile

is some average value, then we believe that the most plausible variation of  $T_e$  with position can be defined by contours of constant  $T_e$  that increase towards and roughly parallel the general outline of the exposed Brazilian shield (Fig. 7). In this case, the contours of constant  $T_e$  cut across the general topographic trend of the Andes, so that more of the Andes in the bend region (Profiles 4 and 5) rest on flexurally strong lithosphere, with a high  $T_e$ , than in profiles further north or south. This concentric pattern of variation in flexural rigidity around the shield area is similar to that observed for North America [21] where  $T_e$  increases from the thermally young regions of the Basin and Range and the Atlantic

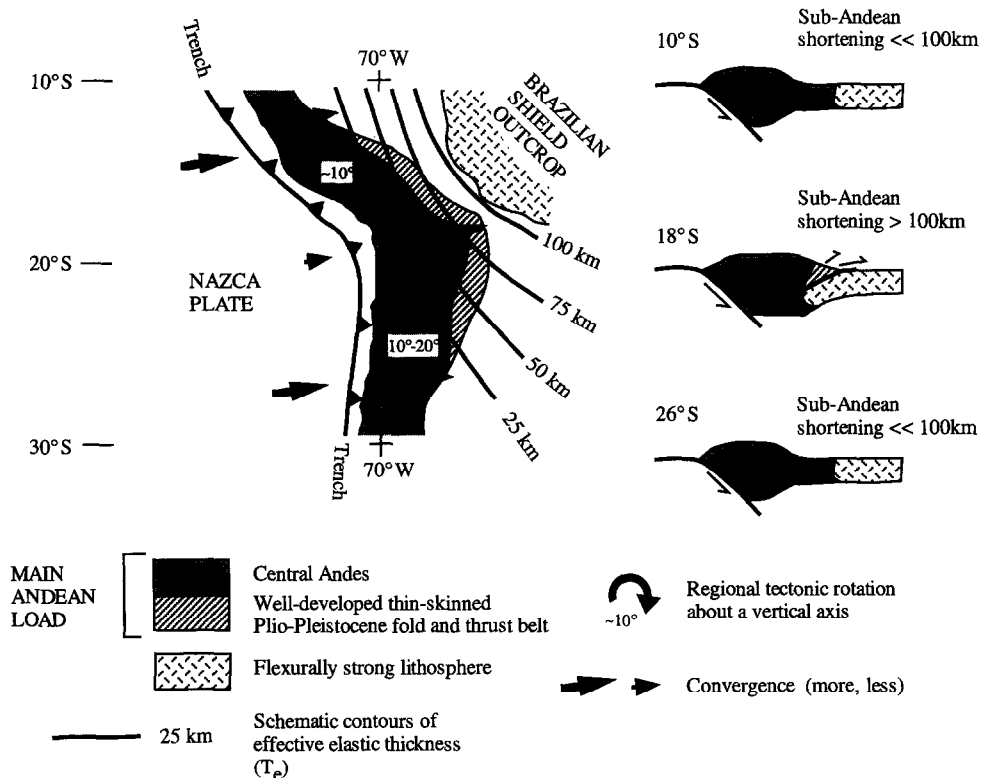


Fig. 7. Schematic diagram showing the relationship between the effective elastic thickness,  $T_e$ , and the amount and nature of shortening in the Central Andes. Contours of  $T_e$  are based on both the gravity modelling illustrated in Figs. 3 and 5 and on the present-day outcrop pattern of the Brazilian shield. Also shown is the part of the Sub-Andes in the bend region where there is a well-developed thin-skinned Plio-Pleistocene fold-and-thrust belt. Curved arrows indicate regional tectonic rotations in the Central Andes since the Middle–Late Miocene based on palaeomagnetic data (see text). Straight arrows illustrate the partitioning of Plio-Pleistocene convergence between that near the trench and that accommodated in the Sub-Andean region. Selected profiles at 10, 18 and 26°S illustrate the general features of Sub-Andean deformation. North and south of the bend (i.e., 10 and 26°S) Sub-Andean deformation is relatively diffuse and involves basement in flexurally 'weak' foreland lithosphere, with less than 100 km of shortening. In the bend region (i.e., 18°S) Sub-Andean deformation involves more than 100 km of underthrusting of a flexurally strong lithosphere.

continental margin to values in excess of 100 km over the Hudson Bay region of the Canadian shield.

Earthquakes [22], seismic reflection profiles and field mapping (unpublished oil company data) [11,9,23,24] all show that the Plio-Pleistocene and active deformation in the Central Andes is concentrated in the Sub-Andean zone. It is striking to us that our proposed regional variations in flexural rigidity of the Central Andes (Fig. 7) correlate with both the nature and amount of shortening in this region. For instance, in the Bolivian Sub-Andes, where we estimate values of  $T_e$  greater than 25 km (Fig. 7), deformation is nearly aseismic and occurs in a thin-skinned fold-and-thrust belt which accommodates underthrusting of the Brazilian shield (unpublished oil company data) [11,23,24]. Estimates of the amount of shortening in the Bolivian Sub-Andean zone increase towards the bend region, with as much as 100–150 km of shortening at the bend (unpublished oil company data) [11,23,24]. In the Sub-Andean zones of Peru and northwestern Argentina [25], further north and south of the bend and where we estimate values of  $T_e$  of less than 25 km, deformation is more complex and involves basement with intense crustal seismicity down to depths of several tens of kilometres. Here, Sub-Andean shortening appears to be much less than 100 km [24].

We believe that the correlation between the spatial variation of the flexural rigidity of the South American Plate and the nature and amount of foreland deformation is significant, although we recognise that there is always a problem in distinguishing cause and effect. We suggest that our observed flexural rigidities are inherited features of the Andean plate margin, pre-dating Cainozoic deformation, and we postulate the following cause and effect relationships with lithospheric deformation. Firstly, the inherited flexural strength of the lithosphere is a principal factor determining the style of lithospheric shortening: high flexural rigidities ( $T_e > 25$  km) promote the initiation and development of thin-skinned fold-and-thrust belts above a basal décollement; low flexural rigidities ( $T_e < 25$  km) promote thick-skinned zones with basement shortening. Secondly, thin-skinned belts are generally an energetically more favourable way of accommodating shortening than thick-skinned zones of deformation that involve basement, perhaps because the geometry of thin-

skinned fold and thrust belts require a smaller cross section of material than the equivalent thick-skinned zone. Thus, where the lithosphere is flexurally strong, foreland deformation tends to be concentrated into a thin-skinned fold-and-thrust belt, above a low-angle basal décollement, which absorbs a larger proportion of the overall shortening budget of the mountain belt compared with foreland regions where the lithosphere is flexurally weak, and deformation is more complex and diffuse, involving basement.

A causal relationship between structural style and flexural rigidity needs to be explained in terms of rheological models [26] for the long-term deformation of the continental lithosphere. In the simplest case, flexural rigidity might be expected to reflect the overall integrated strength of the lithosphere. In this case, we can imagine a progressively deforming zone, which gradually incorporates lithosphere of increasing flexural rigidity and, hence, integrated strength. In weak lithosphere, we might expect fragmentation and decoupling of the brittle crust and ductile flow in the lower crust and mantle, resulting in pervasive lithospheric shortening. However, when the deforming zone eventually impinges on lithosphere with a sufficiently high rigidity and integrated strength, we might expect deformation to become concentrated in a zone at the boundary between 'weak' and 'strong' lithosphere, rather than propagating further into the stronger lithosphere. In this way, a thin-skinned fold-and-thrust belt might be initiated, forming a type of subduction zone that more efficiently accommodates the underthrusting of an interior shield area. The presence of suitable décollement horizons may also promote the development of low-angle thrusts in the toe region of a thin-skinned fold-and-thrust belt. Thus, thick Palaeozoic sedimentary sequences in the bend region of the Bolivian Andes are mainly fine grained and form good décollement horizons. However, we do not believe that the distribution of these sequences could control regional variations in the nature and amount of shortening on a scale of hundreds to thousands of kilometres.

We conclude that variation in flexural strength of the lithosphere, which we believe is a pre-Cainozoic feature of the South American Plate, may have controlled the variation in the amount of Andean foreland shortening by promoting thin-skinned deforma-

tion where the lithosphere is flexurally strong ( $T_c > 25$  km). It is clear to us that the observed along-strike shortening gradients in the Sub-Andean zone have accommodated regional rotation about a vertical axis of the *entire* width of the Central Andes, west of the Sub-Andean zone, relative to stable South America (Fig. 7). This rotation has occurred since the Late Miocene, when deformation in the Sub-Andean zone was most active. Thus, palaeomagnetic data show that, south of the bend, the Andes have rotated regionally about a vertical axis up to 30° clockwise relative to stable South America since the Late Miocene [27,28] [S.H. Lamb, unpublished data]. Similarly, a regional anticlockwise rotation about a vertical axis up to 20° since the Middle Miocene has been observed in palaeomagnetic data north of the bend [27,29] [S.H. Lamb, unpublished data]. Consequently, the previous discussion suggests that regional variations in flexural rigidity have controlled the bending of the *entire* mountain belt. Although we have only considered here the Late Miocene and younger deformation in the Sub-Andean zone, it is possible that this relationship between the flexural strength and Andean deformation also applies to the longer term Tertiary history. If this is the case, the flexural rigidity of the lithosphere is a critical factor in understanding the large-scale development of mountain belts in convergent plate boundaries.

### Acknowledgements

We thank P. Molnar for his critical comments on an early version of the paper and T. Jordan and M. McNutt for their reviews. [CL]

### References

- [1] W.A. Heiskanen and F.A. Vening-Meinesz, *The Earth and its Gravity Field*, 470 pp., McGraw-Hill, New York, 1958.
- [2] G.P. Woollard, Regional variations in gravity, in: *The Earth's Crust and Upper Mantle*, P.J. Hart, ed., Am. Geophys. Union Monogr. 13, 1969.
- [3] G.D. Karner and A.B. Watts, Gravity anomalies and flexure of the lithosphere at mountain ranges, *J. Geophys. Res.* 88, 10449–10477, 1983.
- [4] H. Lyon-Caen, P. Molnar and G. Suárez, Gravity anomalies and flexure of the Brazilian shield beneath the Bolivian Andes, *Earth Planet. Sci. Lett.* 75, 81–92, 1985.
- [5] L. Royden, The tectonic expression of slab pull at convergent plate boundaries, *Tectonics* 12, 303–325, 1993.
- [6] P.C. England and D.P. McKenzie, A thin viscous sheet model for continental deformation, *Geophys. J. R. Astron. Soc.* 70, 295–321, 1982.
- [7] P.C. England and G. Houseman, Finite strain calculations of continental deformation 2. Comparison with the India–Asia collision zone, *J. Geophys. Res.* 91, 3664–3676, 1986.
- [8] C. Demets, R.G. Gordon, D.F. Argus and S. Stein, Current plate motions, *Geophys. J. Int.* 101, 425–478, 1990.
- [9] J. Dewey and S.H. Lamb, Active Tectonics of the Andes, *Tectonophysics* 205, 79–95, 1992.
- [10] B.L. Isacks, Uplift of the central Andean plateau and bending of the Bolivian orocline, *J. Geophys. Res.* 93, 3211–3231, 1988.
- [11] T. Roeder, Archaeo-age structure of Eastern Cordillera in the Province of La Paz, Bolivia, *Tectonics* 7, 23–39, 1988.
- [12] S. Strunk, Analyse und Interpretation des Schwerefelds des activen Kontinentalrandes der zentralen Andes, Ph.D Thesis, Free Univ., Berlin, 1990.
- [13] D. Whitman, Moho geometry beneath the eastern margin of the Andes, northwest Argentina: Constraints on the elastic thickness of the Andean foreland, *J. Geophys. Res.*, in press.
- [14] C.M. Green and J.D. Fairhead, The South American Gravity Project, in: *Recent Geodetic and Gravimetric Research in Latin America*, W. Torge, A.G. Fletcher and J.G. Tanner, eds., pp. 82–95, Springer, Vienna, 1991.
- [15] P. Wessel and W.H.F. Smith, Free software helps map and display data, *Eos* 72, 441–446, 1991.
- [16] M. Gurnis, Ridge spreading, subduction, and sea level fluctuations, *Science* 250, 970–972, 1990.
- [17] T. Cahill and B.L. Isacks, Seismicity and shape of the subducted Nazca plate, *J. Geophys. Res.* 97, 17503–17529, 1992.
- [18] T.E. Jordan, Thrust loads and foreland basin evolution, Cretaceous, western United States, *Am. Assoc. Pet. Geol. Bull.* 65, 2506–2520, 1981.
- [19] C. Beaumont, Foreland basins, *Geophys. J. R. Astron. Soc.* 65, 291–329, 1981.
- [20] T.C. Hanks, The Kuril trench–Hokkaido rise system: Large shallow earthquakes and simple models of deformation, *Geophys. J. R. Astron. Soc.* 23, 173–189, 1971.
- [21] T.D. Bechtel, D.W. Forsyth, V.L. Sharpton and R.A.F. Grieve, Variations in effective elastic thickness of the North American lithosphere, *Nature* 343, 636–638, 1990.
- [22] ISC and Harvard moment catalogues.
- [23] B. Sheffels, Lower bound on the amount of crustal shortening in the central Bolivian Andes, *Geology* 18, 812–815, 1990.
- [24] P. Baby, B. Guillier, J. Oller, G. Herail, G. Montemurro, D. Zubieta and M. Specht, Structural synthesis of the Bolivian Subandean Zone, 2nd Int. Symp. Andean Geodynamics (Oxford, UK), pp. 159–162, 1993.
- [25] R.W. Allmendinger, V.A. Ramos, T.E. Jordan, M. Palma and B.L. Isacks, Paleogeography and Andean structural geometry, northwest Argentina, *Tectonics* 2, 1–16, 1983.

- [26] E.B. Burov and M. Diament, The effective elastic thickness ( $T_e$ ) of continental lithosphere: What does it really mean?, *J. Geophys. Res.* 100, 3895–3904, 1995.
- [27] B.J. MacFadden, F. Anaya, H. Perez, C.W. Naeser and P.K. Zeitler, Late Cenozoic paleomagnetism and chronology of Andean basins of Bolivia: evidence for possible oroclinal bending, *J. Geol.* 98, 541–555, 1990.
- [28] P. Roperch, M. Fornari and G. Herail, A paleomagnetic study of the Altiplano, 2nd Int. Symp. Andean Geodynamics (Oxford, UK), pp. 241–244, 1993.
- [29] O. Macedo-Sanchez, J. Surmont, C. Kissel and C. Laj, New temporal constraints on the rotation of the Peruvian Central Andes obtained from paleomagnetism, *Geophys. Res. Lett.* 19, 1875–1878, 1992.